



Experimental Investigation of a Condensation Particle Counter Challenged by Particles with Varying Wettability to Working Liquid

Longfei Chen¹, Xin Zhang¹, Cuiqi Zhang¹, Mohsin Raza¹, Xinghua Li^{2*}

¹ School of Energy and Power Engineering, Beihang University, Beijing 100191, China

² School of Space and Environment, Beihang University, Beijing 100191, China

ABSTRACT

The counting efficiency of an in-house laminar flow Condensation Particle Counter (CPC) was investigated experimentally. The CPC was challenged by different sources of particles (ambient particles, and combustion particles generated from CH₄ and C₂H₄), and the counting efficiency of the in-house ultrafine CPC (IUCPC) was obtained by comparing particle concentration data measured by the IUCPC with that measured by a reference instrument, TSI CPC 3775. The counting efficiency is closely related to the contact angle (an indication of the wettability of particles by the working fluid) and the combination of the saturator and the condenser temperatures. The particles from different sources appeared to have different contact angles, in other words, different wettability by the working liquid.

Keywords: Condensation particle counter; Counting efficiency; Wettability.

INTRODUCTION

The adverse effects of vehicular emissions, especially particulate matter emissions on health and environment have triggered research interests in fuel formulations (Chen *et al.*, 2012b; Giakoumis *et al.*, 2012; Millo *et al.*, 2012; Chen *et al.*, 2015; Amara *et al.*, 2016), engine calibration and designs (Chen *et al.*, 2012a; Lee and Jeong, 2012; Tan *et al.*, 2014; Chen *et al.*, 2017), and effective after treatment technologies (Mamakos *et al.*, 2013b; Lee *et al.*, 2015) to reduce ultrafine particle emissions. Increasingly stringent regulations such as Euro 5/6 legislation, which specifies a non-volatile particle number emission limit of 6×10^{11} particles km⁻¹ to complement the mass-based limit for particulate emissions from light-duty diesel vehicles, have been proposed (Giechaskiel *et al.*, 2011; Otsuki *et al.*, 2014). A reliable and precise method for measuring ultrafine particle number concentrations has been pursued as modern engines become greener. Economic Commission for Europe (ECE) regulation No.83 requires only solid particles to be counted, and samples need to be collected from a full dilution tunnel with a volatile particle remover (VPR) to remove all the volatile and semi-volatile particles prior to counting. Solid particles are then measured by a condensation particle counter (CPC) with the cut-off size (diameter where 50%

sampled particles were detected successfully by instruments, D₅₀) being 23 nm electrical mobility particle diameter (Otsuki *et al.*, 2014).

A CPC detects particles by condensational growth in supersaturated vapor in the condenser and measures scattered light signal from grown particles of optically visible sizes. CPCs can be classified into three types: expansion, laminar flow and mixing. The expansion type CPC was developed as a ‘dust counter’ and ‘nephelescope’ (Espy, 1841; Coulier, 1875; Aitken, 1881). The laminar flow type, comprised of a saturator, a condenser and an optical particle counter (OPC), allows for continuous monitoring. Depending on the Lewis number of working liquid (Le number, the ratio between thermal diffusivity and mass diffusivity), the instruments can be classified into water-based type (Le number < 1) and alcohol-based type (Le number > 1) (Sem, 2002; Biswas *et al.*, 2005; Hering *et al.*, 2005; Petäjä *et al.*, 2006). Often sheath air was introduced to the CPC system to reduce diffusion loss and response time (Stolzenburg and McMurry, 1991; Iida *et al.*, 2008). The mixing type works without the limitation of thermal diffusivity as the super-saturation is created by turbulently mixing warm and cold flows (Hoppel *et al.*, 1979; Kousaka *et al.*, 1982). This study focuses on the laminar alcohol-based type CPC with sheath air, which is the mainstream CPC type.

The particle detection efficiency, one of the most important characteristics of CPCs, depends on a number of factors such as the physical and chemical properties of both working fluid and particles, the structure of CPC, the saturator temperature and the condenser temperature. Previous research revealed that the cut-off size decreased and the particle

* Corresponding author.

Tel.: +86-10-82316160; Fax: +86-10-82314215
E-mail address: lixinghua@buaa.edu.cn

detection efficiency curve became steeper as the temperature difference between the saturator and condenser increased (Mertes *et al.*, 1995; Hermann and Wiedensohler, 2001). Moreover, commercial CPCs with identical nominal cut-off size from different manufactures have different saturator and condenser temperature settings. For two Particle Measurement Programme (PMP) compliant CPCs, the saturator and condenser temperatures of GRIMM model 5430 are 35°C and 26°C, whilst the saturator and condenser temperatures of TSI model 3790 are 38.3°C and 31.7°C respectively (Giechaskiel and Bergmann, 2011). The influences of saturator and condenser temperatures on the CPC performance (e.g., cut-off size and counting efficiency) are proven to be significant, and their effects on the CPC performance need to be investigated further since there is a lack of systematic study on this topic.

Previous researchers have developed numerical models for predicting behavior of specific CPC designs, especially the complex phenomena (involving heat and mass transfer with phase change and homogeneous and heterogeneous growth of ultrafine particles via nucleation and condensation) inside the condenser. Regarding particle activation, most of the existing models utilized the classical Kelvin theory and determined whether the particle can be grown or not by comparing the actual particle size and the derived Kelvin diameter (Winkler *et al.*, 2008; Iida *et al.*, 2009). Apart from particle size, the particle activation also depends on physico-chemical properties of both the particle and the working fluid, which has not been adequately addressed. In other words, few theoretical studies considered the effect of particle chemical composition and its wettability to the working liquid, as it is usually assumed that the Kelvin equation describes adequately the activation process (Stolzenburg and McMurry, 1991). In addition, the Kelvin theory assumes that the particle growth occurs at an infinite rate, which might cause the deviation from the reality especially when the residence time of particles inside the condenser is insufficient for complete particle growth as the actual particle activation rate is not infinite. Therefore, it would be desirable to incorporate a more realistic particle activation theory with the heat and mass transfer model for predicting the complex phenomena within the condenser.

The effect of wettability of challenging particles on working fluid (both water and butanol) has been investigated by some previous researchers. Hering *et al.* (2005) examined the responses of a laminar-flow water-based CPC to different types of challenging particles. They found that inorganic aerosols (sodium chloride, ammonium nitrate, ammonium sulfate) exhibited similar counting efficiency curves for both butanol-based (UCPC reference) and water-based CPC with D_{50} being around 3.5–5 nm. Sodium chloride particles are the most soluble to water, and thus has the smallest activation particle size due to the reduction of the equilibrium vapor pressure caused by water take-up of salt particles. Compared with organic particles (dioctyl sebacate, oleic acid), the cut-off size of the water-based CPC was much larger than for inorganic particles. The D_{50} for dioctyl sebacate particles was around 30 nm, which could be reduced to 13 nm by adding 4 ppt NaCl contaminant. Hakala *et al.* (2013)

investigated into the performance of a water-based CPC TSI 3783 challenged by hygroscopic, water-soluble particles and hydrophobic, insoluble particles. The silver-water contact angle was found to be in the range of 29–45° depending on the temperature difference between the conditioner and the growth tube while the contact angles were 25° and 21° for ammonium sulfate and sodium chloride particles. Liu *et al.* (2006) investigated the performance of three commercially available TSI water-based CPCs for several types of aerosol of known compositions and ambient particles. For the TSI 3785 model, D_{50} was determined to be 3.1 nm for salt particles, 4.7 nm for sucrose and ambient particles, 5.6 nm for silver particles, and > 50 nm for ultrapure oil particles. The sensitivity to oil droplets increased dramatically ($D_{50} < 10$ nm) when the oil was slightly contaminated, which was consistent with Hering's work (Hering *et al.*, 2005). The effect of particle chemical composition on the counting efficiency of a butanol-based CPC was investigated by Giechaskiel *et al.* (2011), and the results reveal that the average n-butanol microscopic contact angle on diesel exhaust and CAST soot was 5–10°, 25° on thermally pre-treated tetracontane particles, and 15–20° on dry sodium chloride particle. In the study of Mamakos *et al.* (2013), the saturator-condenser temperature differences of two butanol-base CPCs were set to be from 5.6 to 11.3°C, and heterogeneous nucleation theory was found to be able to predict the measured counting efficiencies. Poly-alpha-olefin, C14, C16 particles were found to be perfectly wettable particles, while the graphite data could only be reproduced with a contact angle of 6–12°, for all temperatures examined. Both Giechaskiel *et al.* (2011) and Mamakos *et al.* (2013) found that the counting efficiency became more sensitive to particle composition at lower saturator-condenser differences.

In this study, several factors influencing the CPC counting efficiency (saturator temperature, condenser temperature, and different sources of particles with varying wettability to the working liquid) have been investigated experimentally. Particle sources included ambient air particles and solid particles emitted from a gaseous burner.

METHODOLOGY

CPC Working Principle

An in-house ultrafine condensation particle counter (IUCPC) was utilized in this study as shown in Fig. 1. The CPC comprises of three primary parts: the saturator, the condenser, and the optical particle counter (OPC). A similar CPC structure can be found elsewhere in the literature (Collings *et al.*, 2014). Butanol is stored in the saturator as the working fluid while a diesel particle filter (DPF) with a porous structure is used in the saturator to serve as a wick thus making the sheath gas fully saturated. The condenser has a 5 mm diameter and 10 cm long inner cylindrical hole, which retains a lower temperature than the saturator using a thermo-electrical device. Sheath air is saturated with butanol in the saturator to achieve super-saturation via cooling in the condenser. In the optical particle counter (OPC), the conjunction area of the air flow region and optical path is referred to as sensitive volume. When large

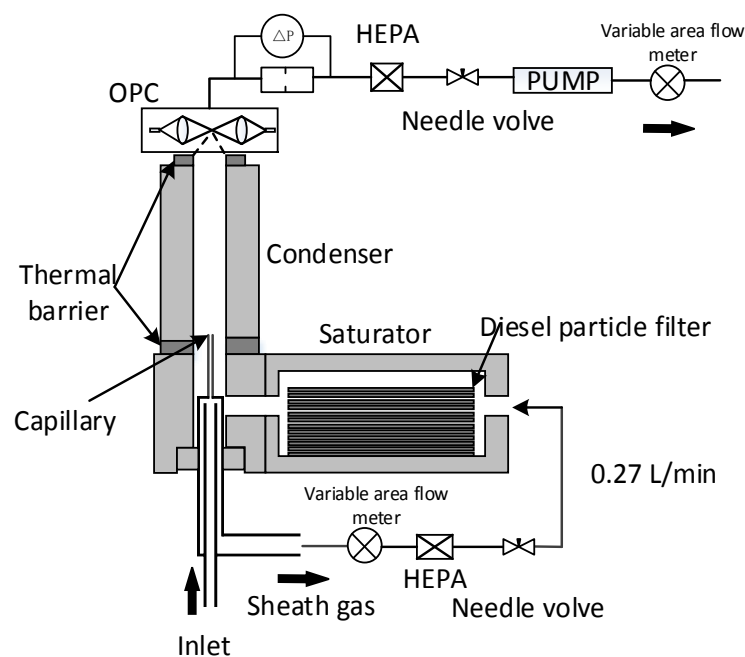


Fig. 1. The schematic diagram of the laminar flow cooling type CPC.

particles traverse this area, Mie-scattering light can be focused by lens to a photodiode, thus pulses are generated and counted. The optical particle counter (OPC) used in this work is a Huayu CLJ-E301 OPC, a sensor which is designed to detect dust particles larger than 0.3 micrometer. More detailed description of the IUCPC can be found in the literature (Chen *et al.*, 2016).

Only a small portion of sampled gas directly flows into the condenser through a capillary while the rest is filtered by a High Efficiency Particulate Air filter (HEPA) and is then saturated with working fluid in the saturator before entering the condenser as shown in Fig. 1.

The flow rate of aerosol flow (in capillary) and total flow was set to be 0.03 L min^{-1} and 0.3 L min^{-1} , and this was achieved by adjusting the opening of two needle valves. The capillary flow rate was determined by taking the difference of the total and sheath flow rates which were monitored by two variable area flow meters. A bubble flow meter (Gilibrator-2) with a resolution of 0.1 mL min^{-1} was used to calibrate the total and sheath flow rates. To ensure that the flow rates were stable, a pressure drop flow meter (SMART SENSOR AS510) along with a 0.4 mm orifice was placed in the in-house CPC as well.

Test Procedure

Fig. 2 shows the schematic of the test rig for measuring the counting efficiency of the in-house CPC. Three types of particles (namely CH_4 combustion particles, C_2H_4 combustion particles and ambient particles) were tested in this work. CH_4 and C_2H_4 gas were burned in a Bunsen burner (Nasco Product Number: SB17085M) and a small amount of air was mixed with CH_4 and C_2H_4 gas by adjusting the slot openings at the base of the barrel in order to generate more combustion particles. The burner flame was contained by a metal collecting cover so that the generated particle emissions

were stable. The sample gas then passed through an ejector diluter so that the temperature cooled down to the CPC operation range. No diluter was needed for sampling the ambient air. Each test point has been repeated for three times with a duration of 10 s and the average results were used for analysis.

Prior to entering the CPCs, large coarse mode particles ($> 1 \mu\text{m}$) were removed by an impactor. Sampled particles then entered through a neutralizer TSI 3077 to form particles with stationary bipolar charge distribution. Mono-disperse negatively charged particles were then obtained when the sample gas flowed through a TSI differential mobility analyzer (DMA) TSI 3081, which was operated in an open-loop with the flow rate of both sheath and excess flows being 6 L min^{-1} . After passing through a T-shape stainless flow splitter, the selected mono-disperse particles were then transported to the IUCPC and a newly calibrated TSI CPC 3775, which has a nominal D_{50} of 4 nm and achieves nearly 100% counting efficiency for particle larger than 10 nm. The TSI 3775 was regarded as a reference instrument and the IUCPC counting efficiency at a given particle size was determined as the ratio of the particle concentration measured by IUCPC to that measured by TSI 3775. Since the flow-rate of the reference instrument and our IUCPC was the same, the effect of the flow splitter on particle concentrations was thought to be insignificant. The outlets to the reference instrument and IUCPC was also swapped to ensure that the same particle size distribution was obtained at different outlets.

The uncertainties of the counting efficiency resulted from several factors: DMA flow error, DMA sizing error, DMA resolution (the ratio of DMA classified particle mean diameter to the full width at half maximum) and the counting errors of both the TSI 3775 and the IUCPC. The sizing error of the DMA was about 3%. The resolution of the DMA was about

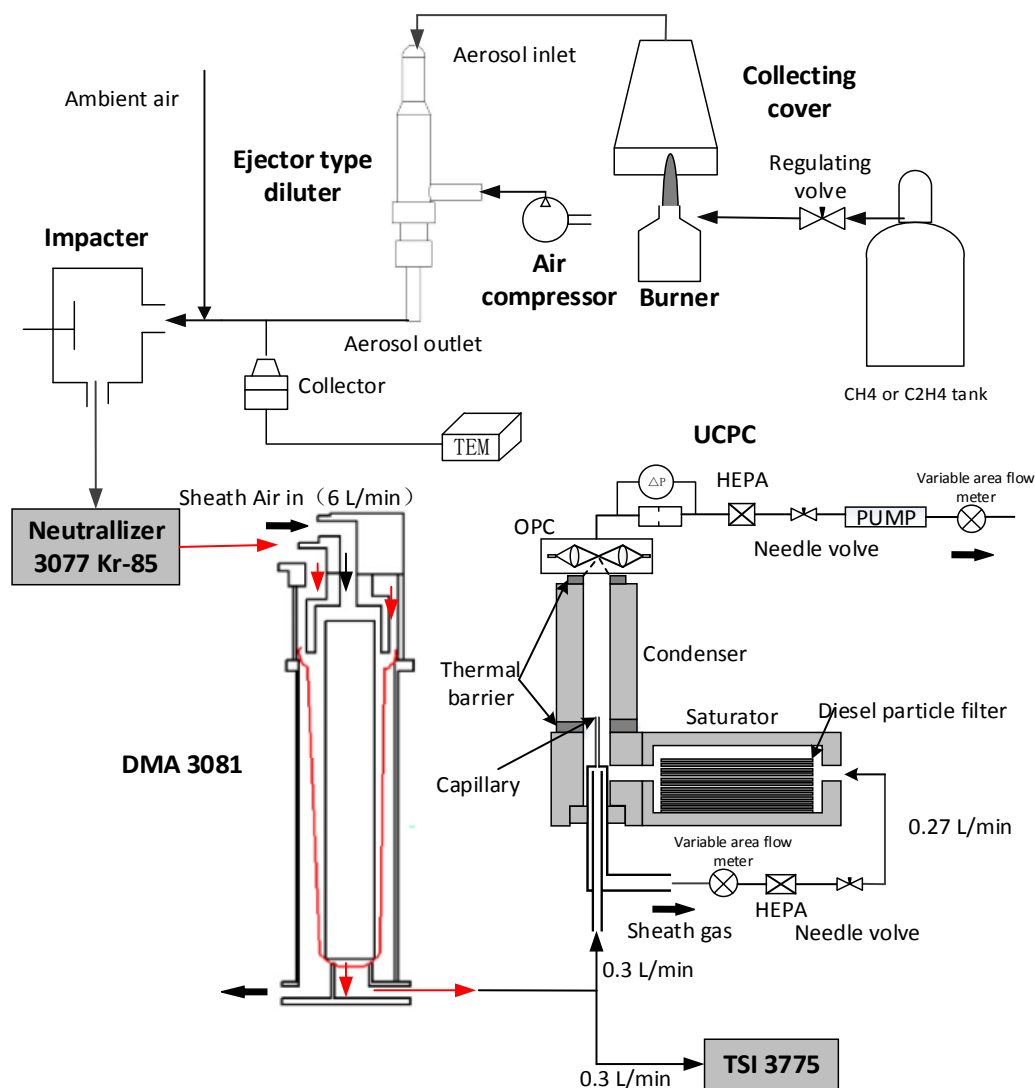


Fig. 2. The schematic of the experimental set-up.

10, which is defined as the reciprocal of the NFWHM (normalized full-width at half-maximum) (Jiang *et al.*, 2011). The uncertainty of the aerosol inlet flow of the TSI 3775 was 5%. The uncertainties of IUCPC flows were determined by the bubble flow meter (Gilibator-2) with a relative accuracy being less than 1%. The uncertainty of the IUCPC was calculated to be about 10%. Detailed uncertainty analysis can be found in another paper (Chen *et al.*, 2016). Before the counting efficiency measurement, the TSI 3775 was connected to the DMA essentially working as a scanning mobility particles sizer (SMPS) to ensure stable particle generation from the burner or the ambient air. Throughout the experiments, homogeneous nucleation (self-condensation of working liquid) was absent, because not a single particle was detected after five-minute counting when the in-house CPC was challenged with HEPA filtered gas.

A separate experiment was carried out to analyze the morphology of CH₄ and C₂H₄ combustion particles, which may provide some insight into how the counting efficiency of IUCPC is influenced by the micro-structure of challenging particles. TEM images are obtained through a JEM-2100F

electron microscope operating at 200 kV using LaB6 filament. The TEM sample was created by dispersing a portion of the collected material from the filter upon TEM grids (400 mesh Copper, Electron Microscopy Sciences).

RESULTS AND DISCUSSION

TEM Images of Combustion Particles

The TEM images of the combustion product of CH₄ and C₂H₄ are presented in Figs. 3 and 4 respectively. The morphology of ambient particles are not presented because of its scarcity and great variation. Most of the CH₄ and C₂H₄ combustion particles are considered as sphere while a small proportion of the combustion particles have a wavy edge. Compared with CH₄ combustion particles, C₂H₄ combustion particles seem to be deviate more from spherical shape. In addition, the agglomerates of C₂H₄ primary particles are more branched and less spherical than the agglomerates of CH₄ primary particles, which means that C₂H₄ particles have larger contact area with the working fluid and thus could be more easily activated in the CPC condenser. The

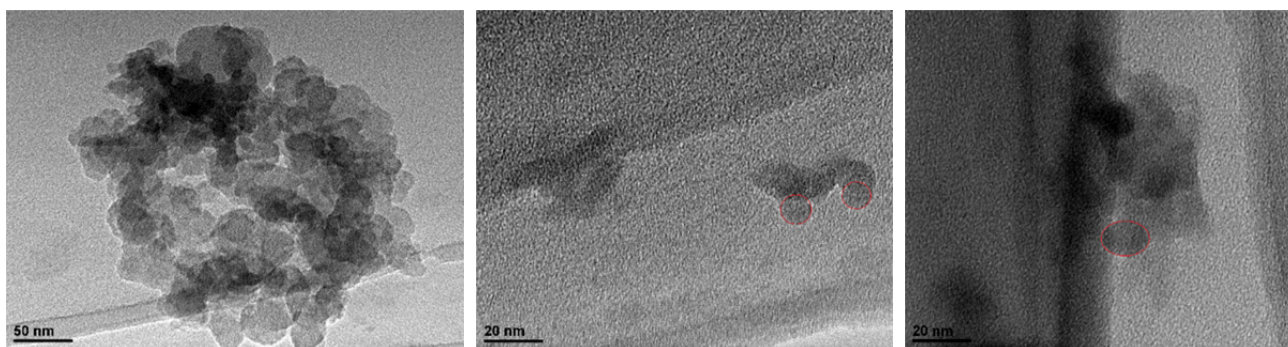


Fig. 3. TEM image of CH₄ combustion particles.

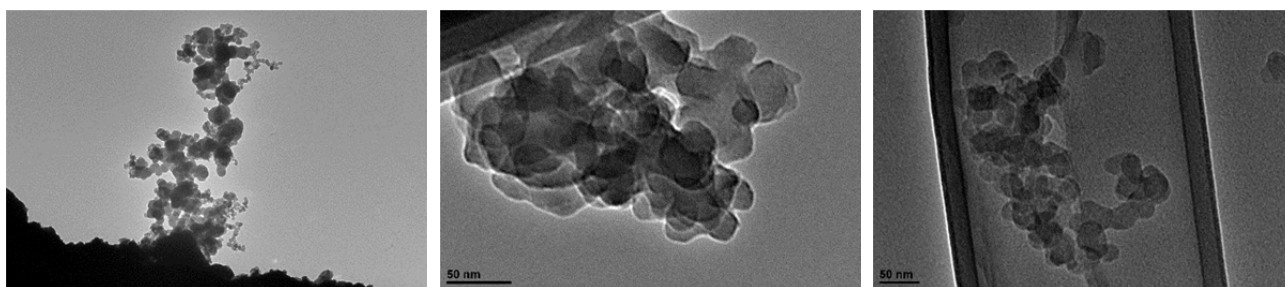


Fig. 4. TEM image of C₂H₄ combustion particles.

different grayscale and fringe pattern of primary particles from different sources imply that CH₄ and C₂H₄ may generate particles of different chemical compositions.

Experimental Counting Efficiencies

Fig. 5 shows the experimental results at $T_s = 38^\circ\text{C}$ and $T_c = 29^\circ\text{C}$ when the IUCPC was challenged with CH₄ and C₂H₄ particles. The counting efficiency increased from 0 to 1 for both CH₄ and C₂H₄ particles as the particle size increased from 13 nm to 19 nm, and C₂H₄ combustion particles exhibited a higher counting efficiency at the same particle size. A plausible reason for the difference of the counting efficiency between CH₄ combustion particles and C₂H₄ combustion particles could be the differences in their hygroscopic properties. The hygroscopic properties of test particles to the working fluid are normally influenced by two factors, namely the composition of test particles and the morphology of the particles. Since particles are not exposed to a high humidity environment before entering the condenser for the sheath flow type CPC, they need to be activated within the period of the time in the condenser, and thus the activation is more easily influenced by the hygroscopic properties of the test particles compared to a full flow type CPC. In general, particles featuring a higher hygroscopic property to the working fluid are more likely to be activated in the condenser.

The difference in the composition of the CH₄ combustion particles and C₂H₄ combustion particles may influence the wettability of the two types of particles with butanol, and thus influence the counting efficiency curve. C₂H₄ is considered to generate more carbonaceous particles than CH₄ because C₂H₄ could form PAHs (Poly-Aromatic Hydrocarbons) relatively easily, which are the soot precursor (Shukla and Koshi, 2012).

The shape of test particles may be another reason contributing to the counting efficiency difference. Compared with ideal spherical particles, non-spherical particles experience higher drag in a differential mobility analyser (DMA), and this will lead to a slight overestimation of their physical size based on their electrical mobility. On the other hand, non-spherical particles may have more contacting line with the working fluid, and thus have higher wettability to the n-butanol. Fig. 6 demonstrates that the experimental counting efficiencies with the temperature difference of 9°C for both conditions $T_s = 31^\circ\text{C}$, $T_c = 22^\circ\text{C}$ and $T_s = 36^\circ\text{C}$, $T_c = 27^\circ\text{C}$. The former case showed a higher overall counting efficiency, which may be due to the non-linear relationship between the saturation pressure of butanol and the temperature. When the temperature difference reduced from 9°C to 6°C , the D_0 (the particle size with which the counting efficiency is just above 0) and D_{50} (cut-off diameter) increased from 12.2 nm, 13.6 nm to 14.8 nm, 17.9 nm, respectively. When the temperature difference was further reduced, the D_{50} increased significantly and was much larger than 23 nm. The results were not shown here because such large cut-off sizes are rarely found in the real applications of CPCs.

Table 1 listed the cut-off size (D_{50}) and the lowest detectable size (D_0) of the IUCPC operating at several working conditions when it is challenged with different particle sources. When the temperature difference of the saturator and the condenser was set to be 9°C , the cut-off size of IUCPC can be found to be more sensitive to the change of the challenging particles as well as the average temperature of the saturator and condenser than the lowest detectable size. The wettability of the ambient particles to working fluid was thought to rank between that of CH₄ combustion particles and C₂H₄ combustion particles.

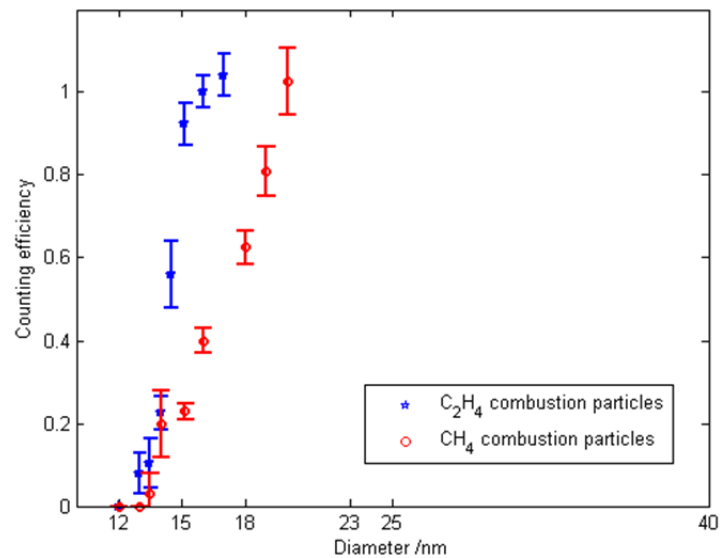


Fig. 5. Experimental counting efficiencies at $T_s = 38^\circ\text{C}$ and $T_c = 29^\circ\text{C}$. Symbols represent the experimental data of CH_4 particles (circle) and C_2H_4 particles (pentagram).

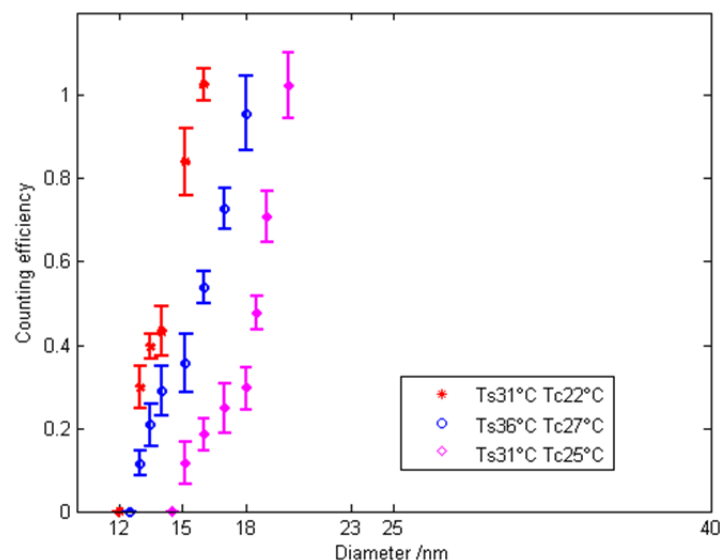


Fig. 6. Experimental (symbols) results of the in-house CPC challenged with ambient air particles at different combinations of the saturator temperature and the condenser temperature.

Table 1. Cut-off diameter (D_{50}) and the lowest observable particles (D_0) for CH_4 , C_2H_4 combustion particles and ambient particles when the IUCPC operating at different combinations of saturator and condenser temperatures

Operating Conditions	Particle source	D_{50}	D_0
$T_s = 38^\circ\text{C}$ $T_c = 29^\circ\text{C}$	CH_4 combustion particles	16.1	13.5
$T_s = 38^\circ\text{C}$ $T_c = 29^\circ\text{C}$	C_2H_4 combustion particles	14.1	12.5
$T_s = 36^\circ\text{C}$ $T_c = 27^\circ\text{C}$	Ambient particles	15.2	12.6
$T_s = 31^\circ\text{C}$ $T_c = 22^\circ\text{C}$	Ambient particles	13.6	12.2
$T_s = 31^\circ\text{C}$ $T_c = 25^\circ\text{C}$	Ambient particles	17.9	14.8

CONCLUSION

A sheath-type CPC was constructed to investigate factors influencing its counting efficiency when challenged with particles from a Bunsen burner and ambient air. The

experiments demonstrated that the counting efficiency is closely linked to the combination of the saturator temperature and the condenser temperature and to the contact angle, which is an indicator of the wettability (or affinity) between particles and the working fluid. When the temperature

difference between the saturator and the condenser remained constant, the counting efficiency curve of the in-house CPC challenged by ambient particles moved left as the average saturator and condenser temperature decreased.

ACKNOWLEDGEMENT

This research is supported by National Natural Science Foundation of China (91641119 and 41575119). This project is also supported by special fund of State Key Joint Laboratory of Environment Simulation and Pollution Control (Grant No. 17K03ESPCP).

SUPPLEMENTARY MATERIAL

Supplementary data associated with this article can be found in the online version at <http://www.aaqr.org>.

REFERENCES

- Agarwal, J.K. and Sem, G.J. (1980). Continuous flow, single-particle-counting condensation nucleus counter. *J. Aerosol Sci.* 11: 343–357.
- Aitken, J. (1881). XII.—On dust, fogs, and clouds. *Trans. R. Soc. Edinburgh* 30: 337–368.
- Amara, A.B., Dauphin, R., Babiker, H., Viollet, Y., Chang, J., Jeuland, N. and Amer, A. (2016). Revisiting diesel fuel formulation from petroleum light and middle refinery streams based on optimized engine behavior. *Fuel* 174: 63–75.
- Biswas, S., Fine, P.M., Geller, M.D., Hering, S.V. and Sioutas, C. (2005). Performance evaluation of a recently developed water-based condensation particle counter. *Aerosol Sci. Technol.* 39: 419–427.
- Chen, L., Stone, R. and Richardson, D. (2012a). Effect of the valve timing and the coolant temperature on particulate emissions from a gasoline direct-injection engine fuelled with gasoline and with a gasoline–ethanol blend. *Proc. Inst. Mech. Eng. Part D* 226: 1419–1430.
- Chen, L., Stone, R. and Richardson, D. (2012b). A study of mixture preparation and PM emissions using a direct injection engine fuelled with stoichiometric gasoline/ethanol blends. *Fuel* 96: 120–130.
- Chen, L., Zhang, Z., Gong, W. and Liang, Z. (2015). Quantifying the effects of fuel compositions on GDI-derived particle emissions using the optimal mixture design of experiments. *Fuel* 154: 252–260.
- Chen, L., Ma, Y., Guo, Y., Zhang, C., Liang, Z. and Zhang, X. (2016). Quantifying the effects of operational parameters on the counting efficiency of a condensation particle counter using response surface Design of Experiments (DoE). *J. Aerosol Sci.* 106: 11–23.
- Chen, L., Liang, Z., Zhang, X. and Shuai, S. (2017). Characterizing particulate matter emissions from GDI and PFI vehicles under transient and cold start conditions. *Fuel* 189: 131–140.
- Collings, N., Rongchai, K. and Symonds, J.P.R. (2014). A condensation particle counter insensitive to volatile particles. *J. Aerosol Sci.* 73: 27–38.
- Coulier, P.J. (1875). Note on a new property of the air. *J. Pharm. Chem.* 22: 165–173.
- Espy, J.P. (1841). *The philosophy of storms*. CC Little and J. Brown, Boston.
- Fletcher, N.H. (1958). Size effect in heterogeneous nucleation. *J. Chem. Phys.* 29: 572.
- Giakoumis, E.G., Rakopoulos, C.D., Dimaratos, A.M. and Rakopoulos, D.C. (2012). Exhaust emissions of diesel engines operating under transient conditions with biodiesel fuel blends. *Prog. Energy Combust. Sci.* 38: 691–715.
- Giechaskiel, B. and Bergmann, A. (2011). Validation of 14 used, re-calibrated and new TSI 3790 condensation particle counters according to the UN-ECE Regulation 83. *J. Aerosol Sci.* 42: 195–203.
- Giechaskiel, B., Wang, X., Gilliland, D. and Drossinos, Y. (2011). The effect of particle chemical composition on the activation probability in n-butanol condensation particle counters. *J. Aerosol Sci.* 42: 20–37.
- Hakala, J., Manninen, H.E., Petäjä, T. and Sipilä, M. (2013). Counting efficiency of a TSI environmental particle counter monitor model 3783. *Aerosol Sci. Technol.* 47: 482–487.
- Hering, S.V., Stolzenburg, M.R., Quant, F.R., Oberreit, D.R. and Keady, P.B. (2005). A laminar-flow, water-based condensation particle counter (WCPC). *Aerosol Sci. Technol.* 39: 659–672.
- Hermann, M. and Wiedensohler, A. (2001). Counting efficiency of condensation particle counters at low-pressures with illustrative data from the upper troposphere. *J. Aerosol Sci.* 32: 975–991.
- Hoppel, W., Twomey, S. and Wojciechowski, T. (1979). A segmented thermal diffusion chamber for continuous measurements of CN. *J. Aerosol Sci.* 10: 369–373.
- Iida, K., Stolzenburg, M.R., McMurry, P.H., Smith, J.N., Quant, F.R., Oberreit, D.R., Keady, P.B., Eiguren-Fernandez, A., Lewis, G.S., Kreisberg, N.M. and Hering, S.V. (2008). An ultrafine, water-based condensation particle counter and its evaluation under field conditions. *Aerosol Sci. Technol.* 42: 862–871.
- Iida, K., Stolzenburg, M.R. and McMurry, P.H. (2009). Effect of working fluid on sub-2 nm particle detection with a laminar flow ultrafine condensation particle counter. *Aerosol Sci. Technol.* 43: 81–96.
- Jiang, J., Attoui, M., Heim, M., Brunelli, N.A., McMurry, P.H., Kasper, G., Flagan, R.C., Giapis, K. and Mouret, G. (2011). Transfer functions and penetrations of five differential mobility analyzers for sub-2 nm particle classification. *Aerosol Sci. Technol.* 45: 480–492.
- Kousaka, Y., Niida, T., Okuyama, K. and Tanaka, H. (1982). Development of a mixing type condensation nucleus counter. *J. Aerosol Sci.* 13: 231–240.
- Kulmala, M., Mordas, G., Petäjä, T., Grönholm, T., Aalto, P.P., Vehkamäki, H., Hienola, A.I., Herrmann, E., Sipilä, M., Riipinen, I., Manninen, H.E., Hämeri, K., Stratmann, F., Bilde, M., Winkler, P.M., Birmili, W. and Wagner, P.E. (2007). The condensation particle counter battery (CPCB): A new tool to investigate the activation properties of nanoparticles. *J. Aerosol Sci.* 38: 289–304.
- Lee, D.W., Hopke, P.K., Rasmussen, D.H., Wang, H.C. and

- Mavliev, R. (2003). Comparison of experimental and theoretical heterogeneous nucleation on ultrafine carbon particles. *J. Phys. Chem. B* 107: 13813–13822.
- Lee, H. and Jeong, Y. (2012). The effect of dynamic operating conditions on nano-particle emissions from a light-duty diesel engine applicable to prime and auxiliary machines on marine vessels. *Int. J. Nav. Archit. Ocean Eng.* 4: 403–411.
- Lee, S., Kwak, J., Lee, S. and Lee, J. (2015). On-road chasing and laboratory measurements of exhaust particle emissions of diesel vehicles equipped with aftertreatment technologies (DPF, urea-SCR). *Int. J. Nav. Archit. Ocean Eng.* 16: 551–559.
- Liu, W., Kaufman, S.L., Osmondson, B.L., Sem, G.J., Quant, F.R. and Oberreit, D.R. (2006). Water-based condensation particle counters for environmental monitoring of ultrafine particles. *J. Air Waste Manage. Assoc.* 56: 444–455.
- Mamakos, A., Giechaskiel, B. and Drossinos, Y. (2013a). Experimental and theoretical investigations of the effect of the calibration aerosol material on the counting efficiencies of TSI 3790 condensation particle counters. *Aerosol Sci. Technol.* 47: 11–21.
- Mamakos, A., Martini, G. and Manfredi, U. (2013b). Assessment of the legislated particle number measurement procedure for a Euro 5 and a Euro 6 compliant diesel passenger cars under regulated and unregulated conditions. *J. Aerosol Sci.* 55: 31–47.
- Mertes, S., Schröder, F. and Wiedensohler, A. (1995). The particle detection efficiency curve of the TSI-3010 CPC as a function of temperature difference between saturator and condenser. *Aerosol Sci. Technol.* 23: 257–261.
- Millo, F., Vezza, D.S., Vlachos, T., De Filippo, A., Ciaravino, C., Russo, N. and Fino, D. (2012). Particle number and size emissions from a small displacement automotive diesel engine: Bioderived vs conventional fossil fuels. *Ind. Eng. Chem. Res.* 51: 7565–7572.
- Otsuki, Y., Takeda, K., Haruta, K. and Mori, N. (2014). A solid particle number measurement system including nanoparticles smaller than 23 nanometers. *SAE Technical Paper* 2014-01-1604.
- Petäjä, T., Mordas, G., Manninen, H., Aalto, P.P., Hämeri, K. and Kulmala, M. (2006). Detection efficiency of a water-based TSI condensation particle counter 3785. *Aerosol Sci. Technol.* 40: 1090–1097.
- Rongchai, K. (2014). *The high temperature condensation particle counter (HT-CPC)—A new instrument for the measurement of solid particulate matter*, Ph. D. thesis, University of Cambridge, Department of Engineering.
- Sem, G.J. (2002). Design and performance characteristics of three continuous-flow condensation particle counters: A summary. *Atmos. Res.* 62: 267–294.
- Shukla, B. and Koshi, M. (2012). A novel route for PAH growth in HACA based mechanisms. *Combust. Flame* 159: 3589–3596.
- Stolzenburg, M.R. and McMurry, P.H. (1991). An ultrafine aerosol condensation nucleus counter. *Aerosol Sci. Technol.* 14: 48–65.
- Tan, P.Q., Ruan, S.S., Hu, Z.Y., Lou, D.M. and Li, H. (2014). Particle number emissions from a light-duty diesel engine with biodiesel fuels under transient-state operating conditions. *Appl. Energy* 113: 22–31.
- Wilson, J., Hyun, J. and Blackshear, E. (1983). The function and response of an improved stratospheric condensation nucleus counter. *J. Geophys. Res.* 88: 6781–6785.
- Winkler, P.M., Vrtala, A. and Wagner, P.E. (2008). Condensation particle counting below 2 nm seed particle diameter and the transition from heterogeneous to homogeneous nucleation. *Atmos. Res.* 90: 125–131.

Received for review, June 11, 2017

Revised, August 25, 2017

Accepted, September 13, 2017